A Helical Twist-induced Conformational Switch Activates Cleavage in the Hammerhead Ribozyme

Christine M. Dunham, James B. Murray and William G. Scott*

Department of Chemistry and Biochemistry, Sinsheimer Laboratories, Center for the Molecular Biology of RNA University of California at Santa Cruz, Santa Cruz, CA 95064, USA

We have captured the structure of a pre-catalytic conformational intermediate of the hammerhead ribozyme using a phosphodiester tether formed between I and Stem II. This phosphodiester tether appears to mimic interactions in the wild-type hammerhead RNA that enable switching between nuclease and ligase activities, both of which are required in the replicative cycles of the satellite RNA viruses from which the hammerhead ribozyme is derived. The structure of this conformational intermediate reveals how the attacking nucleophile is positioned prior to cleavage, and demonstrates how restricting the ability of Stem I to rotate about its helical axis, *via* interactions with Stem II, can inhibit cleavage. Analogous covalent crosslinking experiments have demonstrated that imposing such restrictions on interhelical movement can change the hammerhead ribozyme from a nuclease to a ligase. Taken together, these results permit us to suggest that switching between ligase and nuclease activity is determined by the helical orientation of Stem I relative to Stem II.

© 2003 Published by Elsevier Ltd.

Corresponding author

Introduction

The discoveries that RNA can be an enzyme, and that critically important enzymes such as the ribosome are ribozymes, impel us to answer the question of how ribozymes work in their biological context. The hammerhead ribozyme (Figure 1) is perhaps the simplest and best-characterized ribozyme. Its small size, thoroughly investigated biochemical properties,[1,2] known crystal structures,[3,4] and its biological as well as potential medical relevance,[5] makes the hammerhead ribozyme particularly well-suited to biophysical investigation. The hammerhead ribozyme is derived from a family of small, circular, self-cleaving RNAs that are associated with plant RNA viruses. These satellite RNAs reproduce *via* a rolling-circle mechanism involving formation of linear concatomeric complementary copies of the circular template. The linear concatomers are subsequently cleaved catalytically *via* a phosphodiester isomerization at specific sites that contain the hammerhead RNA sequence to form linear monomers; each linear monomer then possesses a 5′-OH terminus and a 2′,3′-cyclic phosphate terminus. Each linear monomer produced by this process subsequently re-circularizes *via* a ligation reaction catalyzed upon formation of a hammerhead structure comprised of the 5′ and 3′ end sequences of the linear monomer *via* a phosphodiester isomerization that is essentially the cleavage reaction in reverse. Thus the hammerhead ribozyme is derived from an RNA sequence that catalyzes both self-cleavage and self-ligation, depending upon its biological requirements. The mechanism by which the hammerhead RNA switches between the nuclease and ligase activities required during different stages of the satellite virus RNA replication is poorly understood.

The hammerhead ribozyme sequences most frequently studied in the laboratory are ribozymes that greatly favor cleavage over ligation in multiple-turnover reaction assays allowed to establish equilibrium. Recently, it has been found that a previously engineered covalent crosslink[6] between two ribose 2′-oxygen atoms of nucleotides residing in two sequentially distant but spatially proximal locations in the ribozyme crystal structure (residues 2.6 in Stem I and 11.5 in Stem II) shifts the cleavage-ligation equilibrium significantly in such a way that the hammerhead ribozyme becomes a ligase.[7] Further investigation has revealed that a second, similar crosslink (between residues 11.5 and 2.5) produces a hammerhead

E-mail address of the corresponding author: wgscott@chemistry.ucsc.edu
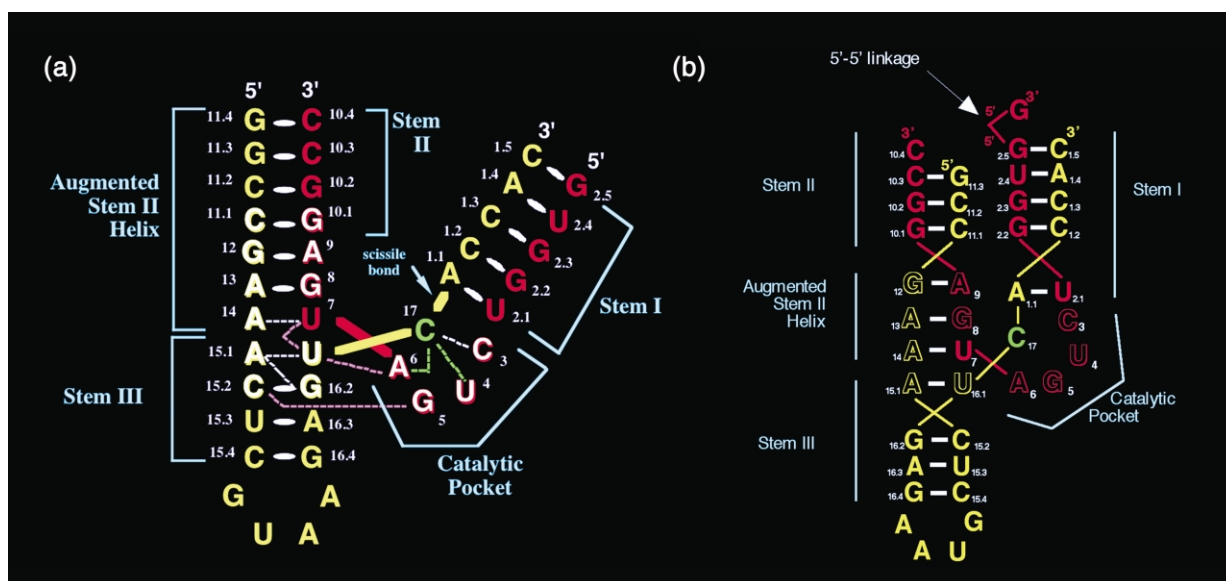
Figure 1. A diagram corresponding to the crystal structure of the initial-state of the hammerhead ribozyme. The enzyme strand is shown in red, the substrate strand in yellow, and the cleavage-site nucleotide, C17, is highlighted in green. The scissile phosphate group lies between C17 and A1.1 as indicated by the arrow. The canonical numbering scheme for the nucleotides and helices is indicated.

RNA that still strongly favors cleavage in its shortest form, but remarkably produces a hammerhead RNA that begins to favor ligation similar to the other crosslink, only when the length of the crosslinking moiety is increased.[8] These results indicate that subtle structural effects, such as the angle and/or relative phase between helical Stem I and Stem II, are likely involved in switching the activity of the hammerhead ribozyme from cleavage to ligation and back, as must be required in the replicative cycle of the satellite RNAs that contain hammerhead RNA sequences.

We are examining the structural basis for ribozyme catalysis in the hammerhead RNA by using a series of X-ray crystallographic freeze-trapping experiments in conjunction with several other structural and biochemical probes. This approach has enabled us to capture four different conformational states of the hammerhead ribozyme on the cleavage reaction pathway, including the initial-state structure,[4] an "early" conformational intermediate[9] in which an approximately 3 Å movement of the scissile phosphate group occurs in conjunction with movement of the cleavage site base and ribose, a larger or "later" conformational change,[10] in which the 2′-oxygen atom attacking nucleophile begins to align with the scissile phosphate group, and finally the structure of the cleaved hammerhead RNA,[11] in the form of an enzyme-product complex held together within the confines of the crystal lattice. These four states have enabled us to produce a simple four-frame "movie" depicting at least a subset of the conformational changes required for catalysis†.

Despite having isolated these individual steps in the reaction pathway, concern remains because: (a) our X-ray diffraction has been limited to 3 Å resolution; (b) additional movements and interactions are likely required (either on a small scale or a large scale) to form the transition-state; and (c) the later conformational change was captured by employing a modified RNA[10] in which an extra methyl group attached to the 5′-carbon atom adjacent to the leaving group oxygen atom presumably interferes with transition-state formation,[12] thus creating a kinetic bottleneck at the bond-breaking stage of the cleavage reaction. Concern has been raised that this modification might have induced formation of an "off-pathway" structural artifact[13] as a consequence of perturbing formation of the transition-state.

Results and Discussion

Structure of a fortuitously tethered hammerhead ribozyme

In order to address the first of these concerns, we attempted to design a more stable crystal packing contact by creating a staggered overlap at the helical interface generated by the crystallographic 2-fold axis (Figure 2(a)). Because the 5′ end of Stem I packs against the 5′ end of Stem II at this interface, we chemically synthesized an RNA possessing an unusual 5′ to 5′ phosphodiester linkage on Stem I, and a corresponding missing nucleotide on Stem II (Figure 2(b)), to facilitate formation of the staggered overlap structure, which we had hoped would stabilize the packing interface, resulting in an increase in the diffraction limit of the crystals.

---

† The movie may be viewed as an animated gif at http://chemistry.ucsc.edu/~wgscott/pubs/movies.html
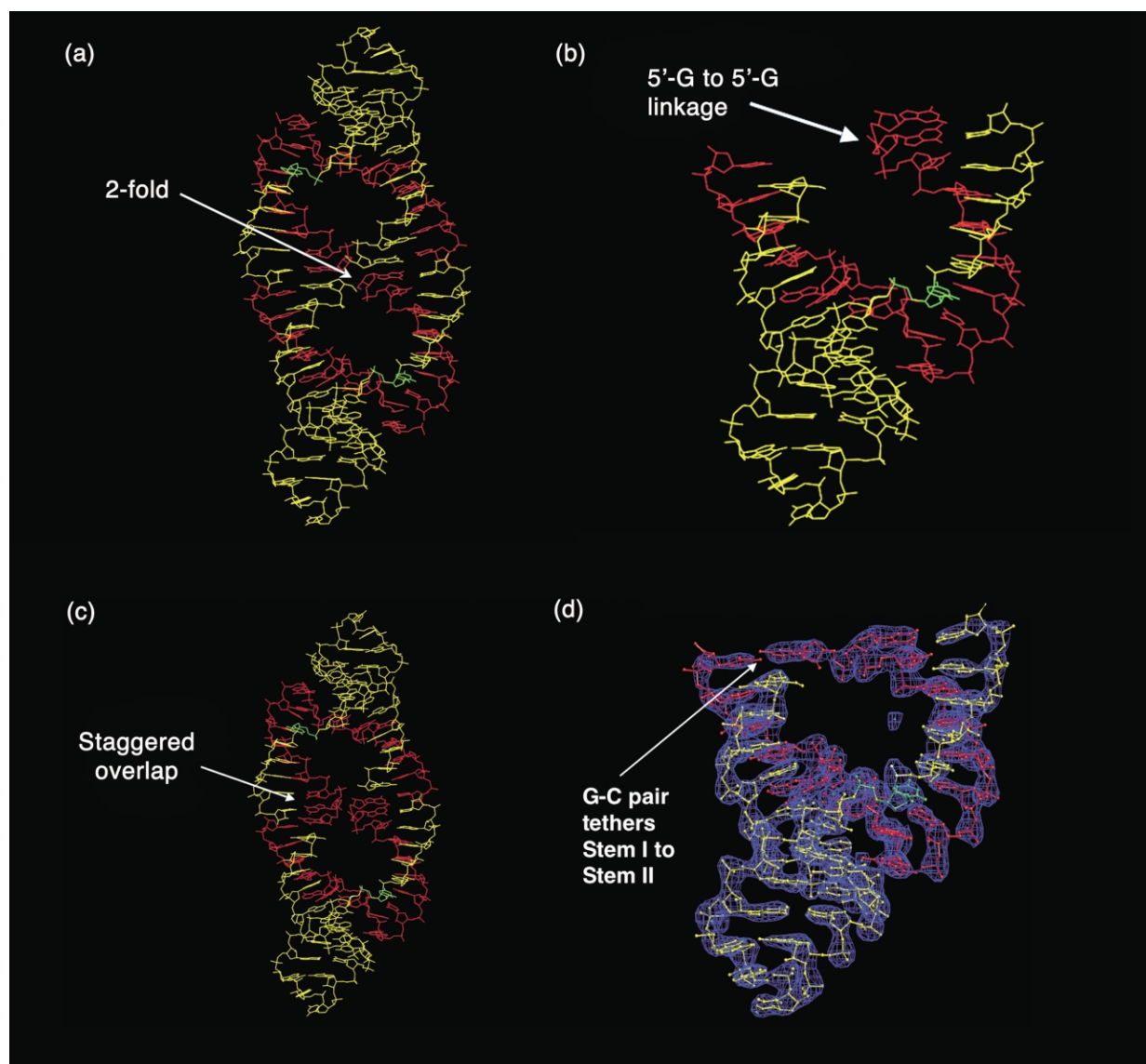
Figure 2. Crystallization of a tethered hammerhead ribozyme. (a) Two molecules in the crystal pack along the crystallographic 2-fold axis, where Stem I of one molecule packs 5′ to 5′ against Stem II of the other. (b) How we attempted to design a better packing interface by removing G11.4 from Stem II and by adding it onto Stem I, with the appropriate orientation facilitated by the 5′ to 5′ phosphodiester linkage, with hopes that the staggered overlap would benefit crystal packing stability at the 2-fold packing interface, as illustrated in (c). However, instead of forming the staggered interface, the extra G base-paired with C10.4, creating a tether between Stems I and II, as shown in (d). The σ-A weighted $2F_o - F_c$ electron density map is contoured above 2.0 times the r.m.s.d. of the map, revealing clear density for the phosphodiester linkage, and a clear gap in the density corresponding to the "missing" phosphodiester linkage between 11.3 and 11.4. These and the following illustrations were made using the OS X native version of PyMol: http://pymol.sourceforge.net/

The modified RNA crystallized readily and the X-ray diffraction data indeed revealed a modest increase in resolution. However, when we solved the structure, we discovered that instead of forming the predicted structure in which the guanosine base linked 5′ to 5′ to the end of Stem I in one molecule formed a staggered overlap with Stem II of a symmetry mate (Figure 2(c)), the unusually linked guanosine base on Stem I instead formed a tethered structure with Stem II within the same RNA molecule (Figure 2(d)). The base of the extra guanosine nucleotide forms a standard Watson–Crick base-pair with C10.4, filling the gap formed by the absence of G11.4 in Stem II. Although we had set out to address the first of the three objections (3 Å resolution diffraction), our experiments with this unique RNA construct in fact address the second and third objections more directly (albeit serendipitously).

The crystal structure of this tethered hammerhead RNA turned out to be more than just an interesting curiosity; use of this construct in a new crystallographic freeze-trapping experiment has enabled us to obtain a much more significant
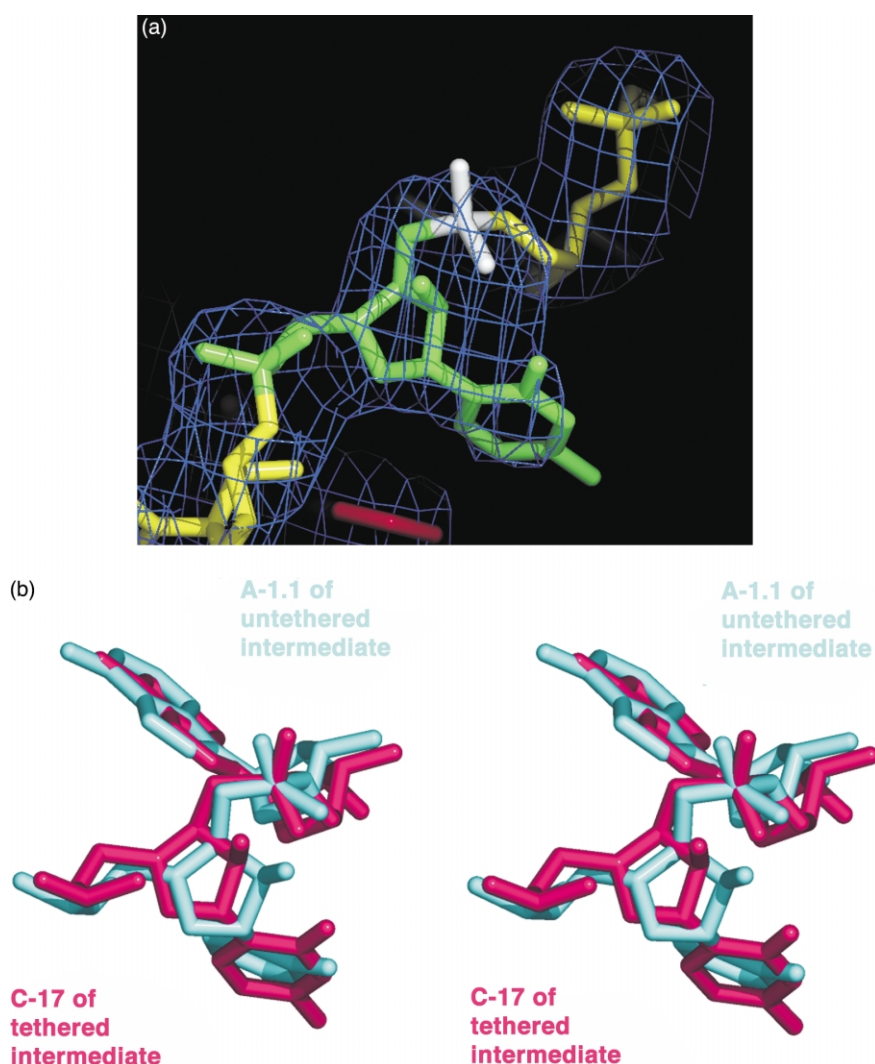
Figure 3. A trapped conformational change. (a) The cleavage site conformational change that aligns the attacking nucleophile of C17 (in green) with the scissile phosphate (in white). About 25° of further rotation of the base and ribose of C17, or a concomitant sugar pucker, will complete the alignment while pushing the 2′ oxygen atom to within bonding distance of the scissile phosphorus atom, presumably in a concerted manner. The σ-A weighted $2F_o - F_c$ electron density map (blue mesh) is contoured above 1.5 times the r.m.s.d. of the map. (b) A comparison of the conformationally changed structure having the Stem I-Stem II tether reported here (magenta) to the previous "late" intermediate structure (cyan) that lacks the tether, showing an overall similarity but suggesting that the new structure reported here is somewhat nearer to the pentacoordinate transition-state structure.

result. We have now captured a further conformational change on the hammerhead ribozyme reaction pathway that precedes cleavage, in a manner that did not require altering the leaving group that might potentially disrupt the transition-state structure or generate an off-pathway artifact. The phosphodiester tether that forms during crystallization of this ribozyme construct inhibits cleavage in the crystal. In solution, the activity of the hammerhead construct pictured in Figure 1(b) is essentially identical to that pictured in Figure 1(a), suggesting that tethering between Stem I and Stem II in solution is negligible. In essence, the phosphodiester tether that forms during crystallization creates a kinetic bottleneck that prevents cleavage from taking place but allows a conformational change that precedes cata-

lysis to take place. This conformational change, which has been trapped using the phosphodiester tether between Stems I and II (Figures 3(a) and (b)), is not only consistent with the previously observed conformational change[10] in which the modified RNA was used to trap the intermediate, but it also appears to be a conformation that is somewhat further along the reaction coordinate (Figure 3(c)), thus revealing at least a subset of the additional torsion angle changes that need to take place in order to form the in-line transition-state during the self-cleavage reaction.

We initiated the cleavage reaction in this second crystal by using conditions identical with those employed previously to capture the structure of the large conformational change preceding catalysis in the hammerhead RNA construct having a

Table 1. Data collection and refinement

Data collection and refinement	Initial-state control	Conformational change
A. *Data collection and processing*		
Resolution range (Å)	100.0–2.85	100–2.99
Data cutoff ($\sigma(F)$)	None	None
Completeness for range (highest shell) (%)	99.3 (99.3)	98.6 (92.8)
No. reflections (highest shell)	8413 (1192)	7686 (1017)
Multiplicity (highest shell)	5.2 (5.3)	5.3 (5.0)
R_{sym} (highest shell)	0.064 (0.316)	0.080 (0.271)
R_{meas} (highest shell)	0.072 (0.349)	0.089 (0.300)
$I/\sigma(I)$ (highest shell)	13.8 (2.2)	9.3 (2.4)
B. *Data used in refinement*		
Resolution range (Å)	19.75–2.85	19.80–3.00
Data cutoff ($\sigma(F)$)	None	None
Completeness for range (%)	99.53	99.3
No. reflections	7544	6872
C. *Fit to data used in refinement*		
Refinement target	Maximum likelihood	Maximum likelihood
Cross-validation method	Throughout	Throughout
Free R value test set selection	Random	Random
R value (working + test set)	0.21	0.23
R value (working set)	0.20	0.23
Free R value	0.23	0.26
Free R value test set size (%)	10.0	10.0
Mean B value (overall, Å²)	41.892	73.011
D. *Correlation coefficients*		
$F_o - F_c$	0.957	0.941
$F_o - F_c$ free	0.939	0.916
E. *rms deviations from ideal values*		
Bond lengths refined atoms (Å)	0.010	0.012
Bond angles refined atoms (deg.)	2.007	2.518

modified leaving group.[10] We raised the pH from 6 to 8.5, slightly above the apparent pK_a of the cleavage reaction, in order to drive most of the RNA molecules within the crystal into the catalytically active state. The rationale for this approach, and our justification for equating the apparent kinetic pK_a with the approximate pK_a of the conformational change, has been addressed.[12] After allowing the crystal to equilibrate at this pH, we flash-froze it in liquid nitrogen and collected data at 100 K, conditions identical with those used to collect data on the control crystal. Data collection and refinement statistics for both crystals are listed in Table 1.

Structure of the trapped intermediate

The crystal structure of the fortuitously tethered hammerhead RNA revealed a rather extensive conformational change at the cleavage site (Figure 3). The tether between Stem I and Stem II, though possibly more strained, remained intact, restricting potential movement of Stem I relative to Stem II (Figure 4). Presumably, this restriction in the movement of Stem I slows or prevents completion of the self-cleavage reaction. Additional movement of the

2′ oxygen atom toward the scissile phosphate group would thus require an accompanying small rigid-body rotation of Stem I about the helical axis. This required movement is presumably prevented by the tether that has formed between Stem I and Stem II. Without the tether present, this particular sequence of RNA cleaves faster, and to a greater degree of completion, within the crystal lattice than it does in solution (Table 2).[10,12]

We assessed the degree to which the new tethered intermediate structure was activated for catalysis by calculating its "in-line fitness", a quantity shown to correlate with phosphodiester cleavage reactivity.[14] The cleavage-site conformation of the intermediate structure of the hammerhead ribozyme was compared to that of the initial-state ribozyme[9] and to that of the previous (untethered) "late" intermediate structure,[10] as well as to three positive controls, in order to quantitate the degree of in-line fitness of the cleavage site (Table 2). An ideal phosphodiester linkage that is perfectly aligned for in-line attack, by definition, possesses an attack angle of 180°; in real cases (the other two controls) the angle is somewhat smaller. If the distance separating the attacking 2′-oxygen and the adjacent phosphorus is 3 Å, such a phosphodiester configuration is assigned an "in-line fitness parameter" of 1.0.[14] The configuration of the phosphodiester linkage at the active site of the hairpin ribozyme[15] is such that the attack angle is 172° and the in-line fitness is 1.3. The G8 to A9 phosphodiester linkage in the hammerhead ribozyme initial-state structure possesses an attack angle of 168° and an in-line fitness of 1.3. The cleavage site of the initial-state structure, which is in an approximate A-form conformation, has an attack angle of only 60° and negligible in-line fitness (0.06). The previously-reported "late" conformational intermediate,[10] which lacks the tether but has a modified leaving group that prevents turnover, has an attack angle of 111° and an in-line fitness of 0.84. The tethered intermediate reported here, by contrast, possesses an attack angle of 135° and an in-line fitness of 1.6. Presumably the tether prevents the additional ~35° orientation required for the phosphate to resemble that of the two real positive controls, yet the in-line fitness parameter is already significantly larger than for either of these more perfectly aligned phosphodiester linkages. This is because the distance between the attacking 2′-oxygen nucleophile and the scissile phosphorus atom is only 2.24 Å, whereas the idealized phosphodiester structure normalizes an in-line fitness of 3.0 Å to a value of 1.0. Apparently, more perfect alignment in the absence of the tether (increase of the attacking angle by another ~35°) will be accompanied by a further reduction of the 2′O to P distance as bond formation occurs.

The hairpin ribozyme favors ligation over cleavage,[15] and the A-9 phosphate of the hammerhead ribozyme does not cleave readily, as we have
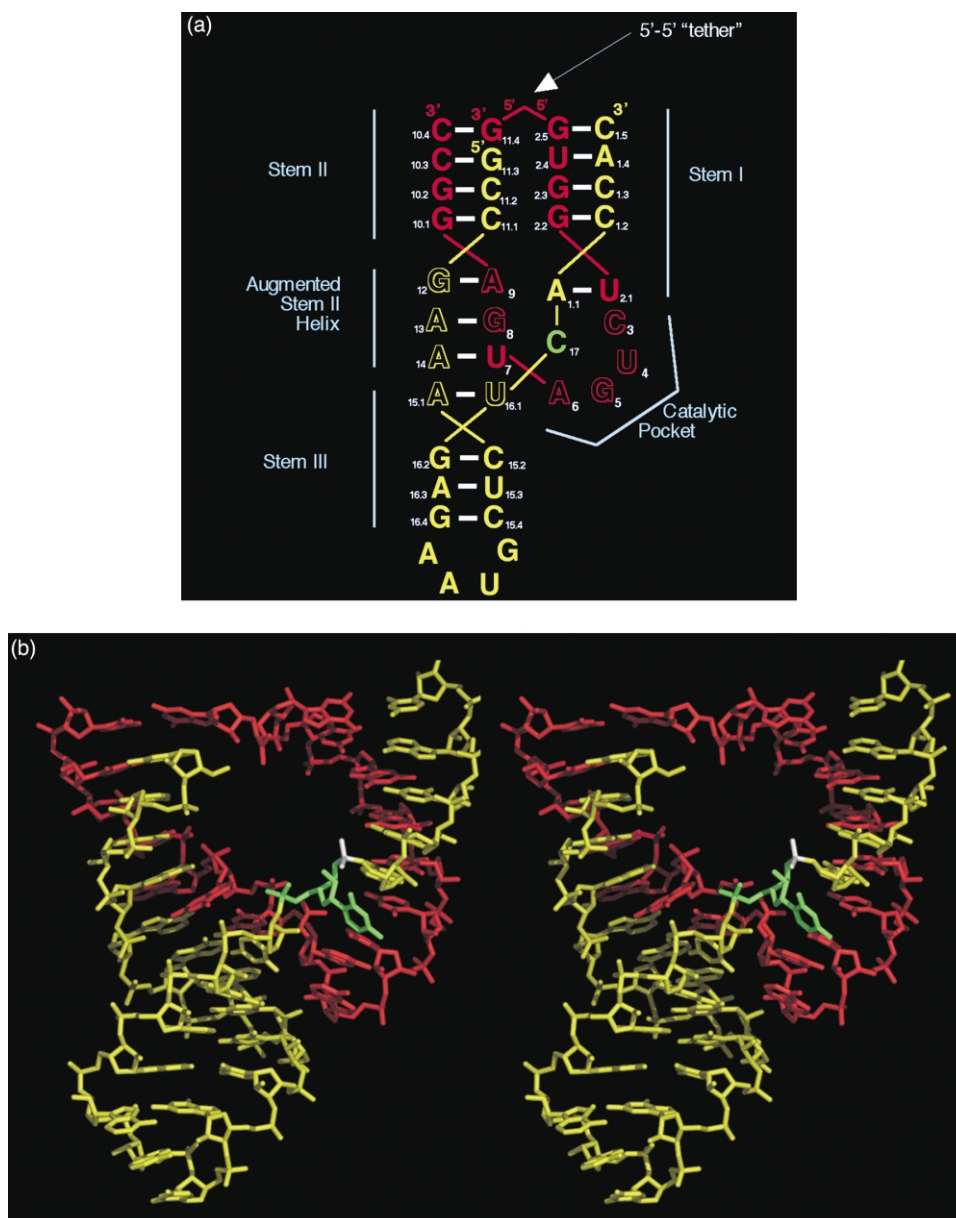
Figure 4 (*legend opposite*)

Table 2. Inter-atomic distances, angles and in-line fitness parameters

Scissile phosphate parameters	Initial-state tethered structure	Untethered intermediate structure	Tethered intermediate structure	A9 phosphate in urx057 structure	"Ideal" in-line structure	Hairpin ribozyme ligation site
d(O2′−O5′) (Å)	3.60	2.51	2.24	2.66	3.00	2.70
d(O2′−O5′) (Å)	1.59	1.59	1.60	1.59	1.59	1.59
d(O2′−O5′) (Å)	3.11	3.42	3.56	4.23	4.59	4.28
In-line angle (deg.)	59.5	111	135	168	180	172
In-line fitness	0.06	0.84	1.6	1.3	1.0	1.3

Scissile phosphate inter-atomic distances, angles, and in-line fitness parameters for the intial-state tethered hammerhead ribozyme structure reported here, the untethered hammerhead ribozyme intermediate structure determined in 1998, the tethered hammerhead ribozyme intermediate structure reported here, as well as the non-cleaving A-9 phosphate site in the hammerhead ribozyme discussed previously,[16] values for Soukup and Breaker's "ideal" in-line phosphate geometry,[14] and values for the active-site structure for the hairpin ribozyme in the ligated form.
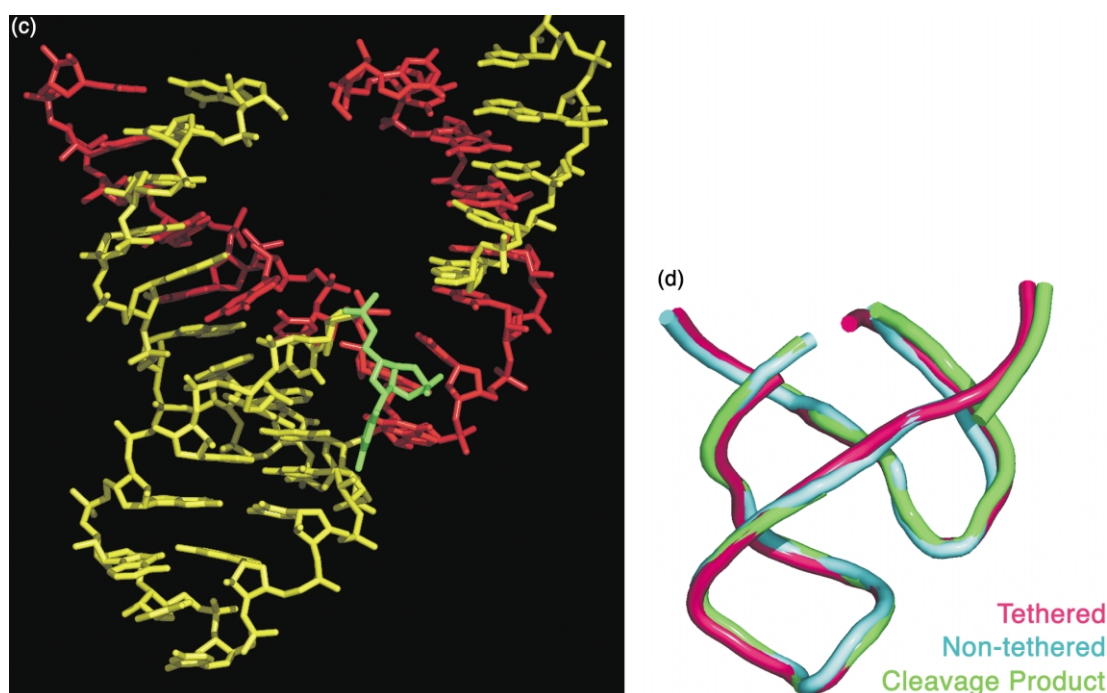
Figure 4. A helical conformational switch accompanies cleavage. (a) Schematic and (b) atomic structures of the tether-trapped intermediate, and (c) the structure of the cleavage product shown in the same orientation. Comparison of (b) to (c) clearly shows that Stem I is oriented differently in the two structures relative to Stem II. (d) A backbone alignment between the tethered-trapped intermediate structure (magenta), the previous late intermediate structure (cyan) that lacked a tether, and the cleavage product structure (green), revealing that the difference in Stem I is due to cleavage of the RNA rather than to the presence (magenta) *versus* the absence (cyan) of the tether, consistent with the interpretation of events given in the text.

described elsewhere.[16] Perhaps the fundamental difference between in-line conformations such as these that stabilize the ligated form of RNA and those that lead to cleaved RNA is that close approach (2.0 to 1.6 Å) of the attacking 2′O nucleophile to the phosphorus atom accompanies angular alignment (the atoms are essentially pushed together, forming a bond) in the case of RNA cleavage, whereas the distance between the 2′O and the P atoms in the ligated RNAs is considerably larger (~2.7 to 3 Å), even after almost perfect angular alignment has occurred (the 2′O at P

atoms are essentially pulled apart). This hypothesis explains why the initial-state structures of the hammerhead RNA, the Pb^{2+}-ribozyme,[17] and tRNA^{PHE} in the presence of Pb^{2+} [18] all share phosphate conformations that are not configured for in-line attack; in each case, alignment could be concomitant with bond cleavage and formation of a 2′,3′-cyclic phosphate product.

Two high-resolution crystal structures of β-phosphoglucomutase[19] reveal apparently stable pentacovalent oxyphosphorane intermediates in which the enzyme active site combined with

Table 3. Stem I tilt, roll and curvature of the tethered intermediate and cleavage product

Stem I helical position	Tilt tethered intermediate	Roll tethered intermediate	Curvature tethered intermediate	Tilt cleavage product	Roll cleavage product	Curvature cleavage product
4/5	−2.9100	5.1400	5.9066	2.4800	7.7300	8.1181
3/4	2.8600	3.2500	4.3292	0.18000	1.1400	1.1541
2/3	4.4400	9.9700	10.914	5.4300	2.3200	5.9049
1/2	−5.6600	1.9400	5.9832	5.7500	−4.9800	7.6068
Mean	−0.3175	5.075	6.7832	3.46	1.5525	5.696
Median	−0.025	4.195	5.9449	3.955	1.73	6.7558
Sum	−1.27	20.3	27.133	13.84	6.21	22.784
Sd. dev.	4.7607	3.5178	2.8574	2.6359	5.2152	3.1723

Summary of RNA helical curvature parameters for the hammerhead ribozyme Stem I, comparing the tethered intermediate structure with that of the cleavage product. The curvature in both cases is fairly similar, although the curvature is somewhat less pronounced subsequent to cleavage, consistent with introducing an extra degree of freedom in the form of a single phosphodiester bond breakage. A comparison of Stem I helical twist in the two structures is shown in Figure 5, together with an approximately 10° change in the orientation of the Stem I helix axis upon cleavage. Helical parameters for this Table and the accompanying Figure 5 were calculated using the program Curves.
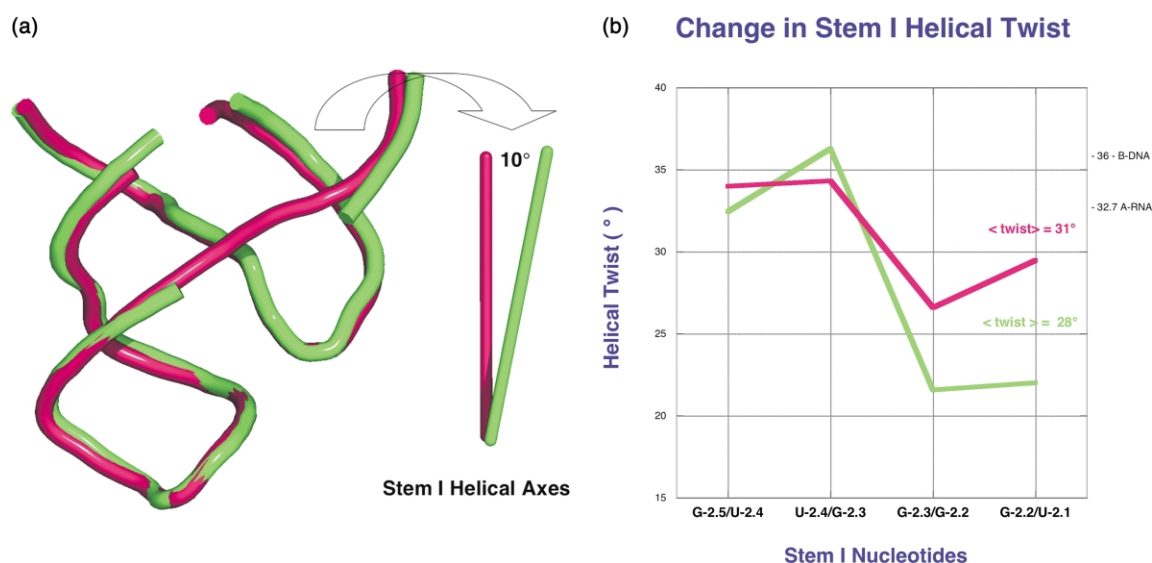
(a)

(b) Change in Stem I Helical Twist

Figure 5. (a) A comparison of Stem I helical twist in the two structures is shown, with the tethered intermediate (magenta) superimposed upon the cleavage product (green). The helical axis of Stem I from each of the two structures was fit to a line using the nucleic acid geometry analysis program Curves, and the angle between these axes was calculated to be approximately 10°. (b) Helical twist parameters for Stem I of the tethered intermediate and cleavage product structures were also calculated using Curves. The motion of Stem I that accompanies cleavage can thus be characterized as an approximately 10° bend with respect to Stem II and Stem III, as well as a small but significant (overall 3° per base-pair or 15° unwinding) of Stem I upon cleavage. The unwinding is most pronounced at the cleavage site. It is fairly likely these differences would be much greater were it not for the constraints imposed by the crystal lattice.

(presumably) crystal lattice interactions somehow traps and preserves this ordinarily evanescent intermediate. In this case, the angle of attack is 174° and the distance between the attacking oxygen nucleophile and the phosphorus atom is 2 Å, indicating simultaneously significant covalent bonding between the phosphorus and both the attacking and leaving group oxygen atoms. In the case of our tethered intermediate, the combined effects of the tether, the crystal lattice, and the pH 8.5 environment stabilize the conformational change, enabling observation of the pre-catalytic conformational change. At 3 Å resolution, it is not possible to assess the degree of covalent character of the 2′O to P interaction, but the close proximity of the two atoms is suggestive that this conformational intermediate may be, at least to a degree, an intermediate in the chemical step of the cleavage reaction as well.

Comparison of the structures of the conformationally changed intermediate (Figure 4(a)) and cleavage product (Figure 4(b)) reveals that the angle between Stem I and Stem II widens significantly as the RNA is cleaved (Figure 4(c)), and the pitch of the helix changes as well, so that the relative orientation between Stem II and Stem I changes slightly as the RNA cleaves. Comparison of the current conformationally changed intermediate structure with the previously-obtained intermediates, in contrast, shows these structures to be more similar (Table 3, Figure 5). This control demonstrates that the narrower angle is not an artifact due to the presence *versus* absence of the crosslink (Figure 4(c)), but rather is a real change that

accompanies cleavage. It permits us to suggest that the reason the hammerhead RNA does not cleave in the crystals of the tethered ribozyme is that Stem I is prevented from moving relative to Stem II. The tether thus creates a kinetic bottleneck that prevents cleavage by restricting helical motion; however, this bottleneck appears to occur further along the reaction pathway than did that created by the modified leaving group; the 2′ oxygen atom attacking nucleophile in the tethered intermediate structure is more in-line with the scissile phosphate group (Figure 3(c)). Because of this, we believe this to be a structure that represents a point on the reaction coordinate further toward the transition-state, and may even possess a stabilizing interaction between the 2′ oxygen atom and the phosphorus atom now only 2.4 Å away. The five crystal structures now enable us to construct a five-frame movie of the cleavage reaction, which may be viewed in the form of an animated gif†.

Helical twist as a regulatory conformational switch

We have observed that the orientation of Stem I relative to Stem II changes by a small but significant extent (Figure 4(d)) upon cleavage of the hammerhead RNA in the crystal. It is possible, and indeed quite likely, that the extent of this

change is much greater in solution, where crystal lattice packing does not constrain the position of Stem I. Nevertheless, this comparatively small motion observed in the crystal structures that accompanies cleavage (a) is clearly sufficient to allow cleavage to take place, as it takes place within the confines of the crystal lattice,[11] and (b) if constrained further by the presence of the tether observed in our crystal structures, prevents cleavage from occurring. We therefore suggest that the observed change in helical conformation is required for cleavage to take place.

The previous chemical crosslinking studies[7,8] demonstrate clearly that the balance between cleavage and ligation can be affected by both the presence of a crosslink and the inter-helical distance constraints it imposes. It is therefore quite likely that the base-pair-mediated tether formed between Stem I and Stem II in our structure, which restricts both helical motion and cleavage activity, may mimic, at least in part, the same interactions between Stem I and Stem II that are perturbed by the chemical crosslinks reported in the previous studies. The biological significance of these observations is that a structural interaction between Stem I and Stem II in the hammerhead self-cleaving RNA may well constitute a biochemical switch that controls whether the hammerhead motif will function as a nuclease or a ligase. Indeed, there is now compelling evidence for a specific interaction between Stem I and Stem II in the wild-type hammerhead RNA sequence that regulates virusiod replication (A. Khvorova, personal communication).

Hammerhead RNAs are found in several species of circular single-stranded satellite RNAs of plant viruses that replicate *via* the rolling circle mechanism. The linear concatomers generated in the initial half of the replicative cycle must first divide into linear monomeric fragments, a process catalyzed by the hammerhead RNA motif functioning in nuclease mode, followed by circularization of each monomer, a process catalyzed by the hammerhead RNA motif functioning in ligase mode. Interactions that restrict motion between Stem I and Stem II that either facilitate ligation or prevent cleavage, similar to what is observed in the crystal structure and is reported to be perturbed by the chemical crosslinking studies, would aid in switching from the nuclease mode to the ligation mode. For these reasons, we suggest that we have inadvertently elucidated the structural basis for the nuclease-ligase switch in the hammerhead RNA that is required for satellite virus RNA replication.

Materials and Methods

Synthesis and crystallization

RNA phosphoroamidites, including the 5′-G-phos-phoroamidite, were obtained from Chemgenes and the RNA was synthesized and purified as described.[10] Crystals containing the hammerhead ribozyme substrate having the 5′-to-5′ phosphodiester linkage and enzyme strand with G11.4 omitted were grown using crystallization conditions reported previously, i.e. with 1 mM ribozyme in 50 mM sodium acetate (pH 5.0), 1.8 M Li_2SO_4 in the absence of Mg^{2+} and other divalent cations. The various strands of RNA were synthesized using oligoribonucleotide phosphoramidite chemistry, using deoxycytosine solid-phase supports. The RNA was purified successively by anion-exchange HPLC and C-18 reverse-phase HPLC, and subsequently de-salted. Four microliters of the RNA solution were then combined with 2 μl of reservoir solution (50 mM sodium acetate (pH 5.0), 1.8 M Li_2SO_4, 1.0 mM EDTA), and equilibrated as hanging or sitting-drops against 0.75 ml of the reservoir solution sealed in a Linbro tissue-culture plate at 16 °C. The best crystals (0.5 mm × 0.3 mm × 0.3 mm) grew in these initially 6 μl drops rather than larger drops, formed within two to three days.

Collection of X-ray diffraction data

The "control" crystal was soaked in a freezing solution consisting of 20% (v/v) glycerol, 50 mM cacodylic acid (buffered at pH 6.0), 1.8 M Li_2SO_4, 50 mM $CoCl_2$. The conformationally trapped crystal was similarly prepared in a freezing solution consisting of 20% glycerol, 50 mM Tris (buffered at pH 8.5), 1.8 M Li_2SO_4, 50 mM $CoCl_2$ for 120 minutes. In both cases, the soaking experiments were terminated by flash-freezing the crystals in a bath of liquid nitrogen. Further details of data collection are described in Table 1. We assayed the cleavage in the crystal by HPLC as described previously and detected only small amounts of cleavage. Diffraction data were collected at the Advanced Light Source, Beamline 5.0.2 on a ADS CCD detector.

Data processing and crystallographic refinement

The data were processed using MOSFLM and CCP4.[20] Initial rigid-body refinement followed by conventional positional refinement (Powell minimization) in CNS v. 1.1[21] was then performed to refine a starting model (URX057)[9] for each RNA crystal structure, without modifying the RNA to match the sequences of RNA in the present experiments. This starting model was then further refined using a standard simulated annealing slow-cooling molecular dynamics protocol followed by conventional positional and (highly) restrained temperature factor refinement in CNS-1.1 using all of the data. Finally, the RNA was rebuilt when the unusual base-paired phosphodiester tether became apparent, and the modified RNA with the 5′-to-5′ linkage was further refined using CCP4 REFMAC,[22] which greatly facilitated incorporation of the unusual nucleotide linkage. RNA helical parameters (Table 3 and Figure 5) were calculated using the program Curves.[23]

Data Bank accession code

Coordinates have been deposited with the Nucleic Acid Database (accession codes 1NYI and 1Q29) for immediate release.

Acknowledgements

References

1. Stage-Zimmermann, T. K. & Uhlenbeck, O. C. (1998). Hammerhead ribozyme kinetics. *RNA*, **4**, 875–889.
2. McKay, D. B. (1996). Structure and function of the hammerhead ribozyme: an unfinished story. *RNA*, **2**, 395–403.
3. Pley, H. W., Flaherty, K. M. & McKay, D. B. (1994). Three-dimensional structure of a hammerhead ribozyme. *Nature*, **372**, 68–74.
4. Scott, W. G., Finch, J. T. & Klug, A. (1995). The crystal structure of an all-RNA hammerhead ribozyme: a proposed mechanism for RNA catalytic cleavage. *Cell*, **81**, 991–1002.
5. Rossi, J. J. (1997). Therapeutic applications of catalytic antisense RNAs (ribozymes). *Ciba Found. Symp.* **209**, 195–206.
6. Sigurdsson, S. T., Tuschl, T. & Eckstein, F. (1995). Probing RNA tertiary structure: interhelical cross-linking of the hammerhead ribozyme. *RNA*, **1**, 575–583.
7. Stage-Zimmermann, T. K. & Uhlenbeck, O. C. (2001). A covalent crosslink converts the hammerhead ribozyme from a ribonuclease to an RNA ligase. *Nature Struct. Biol.* **8**, 863–867.
8. Blount, K. F. & Uhlenbeck, O. C. (2002). InteRNAl equilibrium of the hammerhead ribozyme is altered by the length of certain covalent cross-links. *Biochemistry*, **41**, 6834–6841.
9. Scott, W. G., Murray, J. B., Arnold, J. R., Stoddard, B. L. & Klug, A. (1996). Capturing the structure of a catalytic RNA intermediate: the hammerhead ribozyme. *Science*, **274**, 2065–2069.
10. Murray, J. B., Terwey, D. P., Maloney, L., Karpeisky, A., Usman, N., Beigelman, L. & Scott, W. G. (1998). The structural basis of hammerhead ribozyme self-cleavage. *Cell*, **92**, 665–673.
11. Murray, J. B., Szoke, H., Szoke, A. & Scott, W. G. (2000). Capture and visualization of a catalytic RNA enzyme-product complex using crystal lattice trapping and X-ray holographic reconstruction. *Mol. Cell*, **5**, 279–287.
12. Murray, J. B., Dunham, C. M. & Scott, W. G. (2002). A pH-dependent conformational change, rather than the chemical step, appears to be rate-limiting in the hammerhead ribozyme cleavage reaction. *J. Mol. Biol.* **315**, 121–130.
13. Wang, S., Karbstein, K., Peracchi, A., Beigelman, L. & Herschlag, D. (1999). Identification of the hammerhead ribozyme metal ion binding site responsible for rescue of the deleterious effect of a cleavage site phosphorothioate. *Biochemistry*, **38**, 14363–14378.
14. Soukup, G. A. & Breaker, R. R. (1999). Relationship between internucleotide linkage geometry and the stability of DNA. *RNA*, **5**, 1308–1325.
15. Rupert, P. B. & Ferre-D'Amare, A. R. (2001). Crystal structure of a hairpin ribozyme-inhibitor complex with implications for catalysis. *Nature*, **410**, 780–786.
16. Scott, W. G. (2001). Ribozyme catalysis via orbital steering. *J. Mol. Biol.*, **311**, 989–999.
17. Wedekind, J. E. & McKay, D. B. (1999). Crystal structure of a lead-dependent ribozyme revealing metal binding sites relevant to catalysis. *Nat. Struct. Biol.*, **6**, 261–268.
18. Brown, R. S., Dewan, J. C. & Klug, A. (1985). Crystallographic and biochemical investigation of the lead(II)-catalyzed hydrolysis of yeast phenylalanine tRNA. *Biochemistry*, **24**, 4785–4801.
19. Lahiri, S. D., Zhang, G., Dunaway-Mariano, D. & Allen, K. N. (2003). The pentacovalent phosphorus intermediate of a phosphoryl transfer reaction. *Science*, **299**, 2067–2071.
20. Collaborative Computational Project, Number 4 (1994). The CCP4 suite: programs for protein crystallography. *Acta Crystallog. sect. D*, **50**, 76–763.
21. Brunger, A. T., Adams, P. D., Clore, G. M., DeLano, W. L., Gros, P., Grosse-Kunstleve, R. W. *et al.* (1998). Crystallography & NMR system: a new software suite for macromolecular structure determination. *Acta Crystallog. sect. D*, **54**, 905–921.
22. Murshudov, G. N., Vagin, A. A. & Dodson, E. J. (1997). Refinement of macromolecular structures by the Maximum-Likelihood Method. *Acta Crystallog. sect. D*, **53**, 240–255.
23. Lavery, R. & Sklenar, H. (1988). The definition of generalized helicoidal parameters and of axis curvature for irregular nucleic acids. *J. Biomol. Struct. Dyn.*, **6**, 63–91.